Constriction Coefficient for Thermal Flux in Microelectronic Interconnection Matrices

Morgane M. Autret, Papa M. Souare, Julien Sylvestre
Interdisciplinary Institute for Technology – 3IT, Université de Sherbrooke, QC, Canada

Abstract:
Background*: The modeling of Controlled Collapse Chips Connections (C4) and other large arrays of parallel components using finite element analysis can be a time consuming process. Simplified models such as flux tube modeling replace the solder joints and the underfill with an equivalent homogeneous layer representing the whole layer. This flux tube model uses a single parameter to represent the heat flux constriction at the entrance and exit areas of solder joints, to calculate the conductivity of the equivalent layer (solder joint and underfill).*
Materials and Methods*: We show that the validity of existing parameterizations for the flux constriction is limited to a few simple geometries like the one of a tube. We further present a study of several tridimensionnal geometrical and material parameters that have an influence on the flux constriction parameter.*
Results*: These parameters include the thickness of the underfill and solder joints layer, the volume of the solder joints, the offset between the center of the top and bottom areas of the solder joint, the variation of the ratio of the conductivity of the solder joint to the conductivity of the underfill, the conductivity of the underfill and the in-plane dimensions of the die and of the underfill.*
Conclusion*: We have shown the effects of all the introduced parameters.*
Key Word*: Thermal management of electronics, Modeling, Mathematical model*

I. Introduction

A better understanding and accurate simulation of thermal transfer through matrices of highly conductive elements embedded in a lower conductivity matrix is required to develop different processes used in microelectronics bonding. Processes such as thermocompression bonding [1] usually require trial and error to determine the best possible settings of time and temperature to be used in a given situation. To reduce the time needed for that process, the temperatures of the different elements during the process need to be assessed quickly. A proper understanding of heat transfer is also needed for the normal operation of flip-chip packages, as the chips dissipate significant heat and their maximum temperature must be properly controlled [2]. More or less complex Finite Element Analysis (FEA) modeling can be used to estimate the temperature fields during thermocompression bonding or during flip-chip operation, for instance [3, 4].

The modeling of the thermal flow in a microelectronic interconnection matrix requires significant calculation times with the increasing amount of interconnections and a decreasing size of the finite elements.

As a result, simplified models which provide results with an acceptable accuracy are highly desirable, to quickly provide the required design data to the designers.

II. Flux Constriction

Multiple studies, including [5] and [6], show that the heat flux is more important in the solder joints than in the underfill, as the conductivity of the solder joints is larger (Figure no. 1). The funneling of the heat flux through the reduced section of the solder joints increases the thermal resistance of the layer. This phenomenon can be parameterized by the non-dimensional variable ψ, which characterizes the flux constriction, $\psi = k_{sj}.\sqrt{A_c}.R_c$, (1) with k_{sj} representing the conductivity of the solder joint, A_c the cylindrical contact area with the solder joint and R_c is the thermal constriction resistance.

Figure no 1: Z flux going through the soldier joint (W.mm-2)
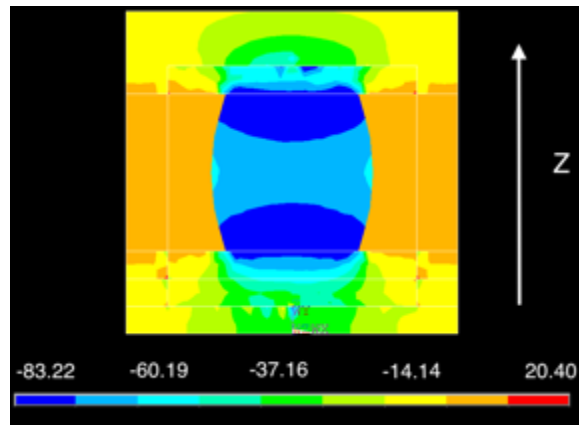
The thermal resistance of a single solder joint is then a function of ψ and is given by $R_{sj} = ((\psi/\sqrt{A_c}).((1/k_L) + \frac{1}{k_D})) + (e/(k_{sj}.A_C))$ (2), where k_L is the conductivity of the substrate, k_D the conductivity of the die and e the thickness of the underfill (or height of the solder joint).

The first term in Eq. 2 represents the thermal resistance from the flux constriction and the second term is the resistance due to the solder material and cylindrical geometry. Assuming that the heat flow is perfectly unidirectional along the z-axis, the total resistance of the portion of the layer comprising a single solder joint and underfill is then obtained with: $(1/R_{eq}) = (1/R_{sj}) + (1/R_u)$ (3), where R_{eq} represents the equivalent total resistance of the layer portion and R_u is the resistance of the underfill volume around the solder joint. In FEA models, the effective thermal resistance of the solder joint matrix-underfill layer, treated as an effective homogeneous material, is then given by $(1/R_{mat}) = \sum(1/R_{eq})$ (4), where R_{mat} represents the thermal resistance of the entire layer of solder joints and underfill, and the sum is over all solder joint regions.

Previous studies have proposed multiple formulas to calculate the value of ψ, using the geometry of the contact areas and the conductivity of the elements constituting the assembly, but these formulas can only be used for simple geometries. For interfaces with imperfect plane surfaces and multiple contact areas, reference [5] provides a definition for ψ by using d_i, the mean diameter of the contact area: $\psi = R_C.2.k_{sj}.d_i$ (5).

According to reference [6], the real geometry can be According to reference [6], the real geometry can be replaced by an equivalent geometry representing a tube which contains all the components to be modeled (die, laminate, underfill, solder joint). The solder joints are represented by either a tube or a rectangular prism with a simple geometry for the contact area (circle/circle, circle/square, square/square). Under such conditions, the authors calculated R_t, the resistance of the whole assembly, knowing the thermal flux Q, applied on the area and the temperature difference ΔT between the two sides, $R_t = (\Delta T/Q)$ (6). The resistances of the die, the laminate and the underfill were then subtracted to obtain R_c. ψ was then calculated for different geometries using Eq. 5. An engineering approximation depending on ε, the ratio of the contact area to the whole area, was obtained by using the different values they calculated and is given by: $\psi = 0.475 - 0.62\varepsilon + 0.12\varepsilon^2$, (7) where ε must be between 0 and 0.5 to provide results with a maximum relative error of 4 percent.

Eq. 7 provides correct results for simple or simplified geometries and it has been a popular choice in the microelectronics modeling literature [7, 8, 9, 10]. However, when the shape of the volumes becomes more complex, like the solder joints shown below in Figures no 3 or no 4, the values provided by Eq. 7 do not give results which are close enough to the results provided by full FEA models of the complete geometry (section 6). To provide a better alternative to using Eq. 7, we did a sensitivity analysis by studying the effects of the variation of a number of parameters on ψ (section 7), and provide values over a variety of configurations which can be used to estimate the equivalent thermal resistance of solder joint-underfill layers in FEA models.

III. Methodology
To provide values of ψ that are well suited to the real geometry of the solder joint, the problem has been approached with the creation of a finite element model including a section of the die, the laminate, the underfill and a single solder joint. A thermal flux was then imposed on the die and the temperature on the laminate was fixed. The temperature of the surface of the die was then extracted from the finite element model. The thermal resistance of the equivalent layer was calculated using Eq. 6 to obtain the total resistance of the assembly. The resistances of the die and of the laminate were then subtracted. The solder joint thermal resistance R_{sj} being the sum of the resistance due to the material of the solder joint and the resistance due to the

flux constriction, the value of ψ was obtained by inverting (2), $\psi = \sqrt{A_c}(1/((1/k_L) + (1/k_D))) \cdot \left(R_{sj} - (e/(k_{sj} \cdot A_c)) \right)$ (8). A simplified model with the thermal resistance extracted from the complete model was then created. The temperature on the surface of the die was extracted to be compared with the temperature from the complete model and from the simplified model using the existing simplified formulas, in order to validate our model.

Then we studied the potential influence of different parameters in the model, including: the thickness of the underfill (with cylindrical interconnects and with solder joint), the volume of the solder joint, the offset between the center of the solder contact on the die and the center of solder contact on the laminate, up to 0.4 mm [11], the difference of conductivity between the solder joint and the underfill as well as the area density of solder joints.

IV. Numerical Model

We used a custom software (PACK [12]) to create the finite numerical model through a virtual platform. This software allowed us, through an object-oriented programming code, to put together the custom microelectronic components or selected ones from databases and generate quickly an Ansys APDL file. The program can then pre-process, solve and post-process the files and extract all the information needed from the model. The PACK software allows complex models to be created by assembling different pre-existing and customizable blocks. PACK has been used for flip-chip modeling and is used for virtual prototyping by the IBM Corporation.

Using PACK, the model was created by assembling a die, a laminate, an underfill and by embedding a solder joint in the underfill. The geometry of the solder joint was created using the software Surface Evolver [13]. A box using a refined mesh was created inside the geometry previously modeled to embed the solder joint, as represented in Figure no 2 for a cylindrical tube or in Figure no 3 for a more realistic geometry to represent a solder joint.
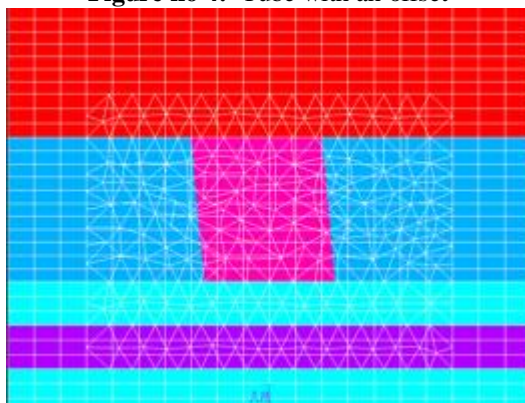
Figure no 2; Simple geometry of a tube
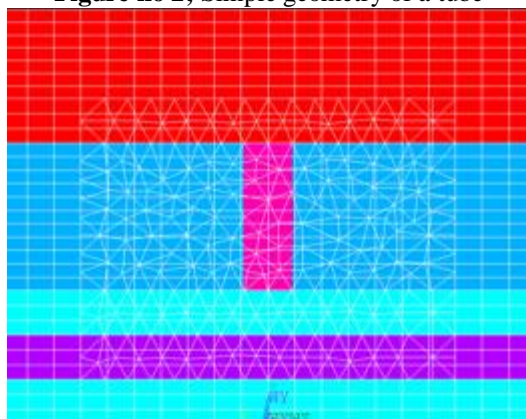
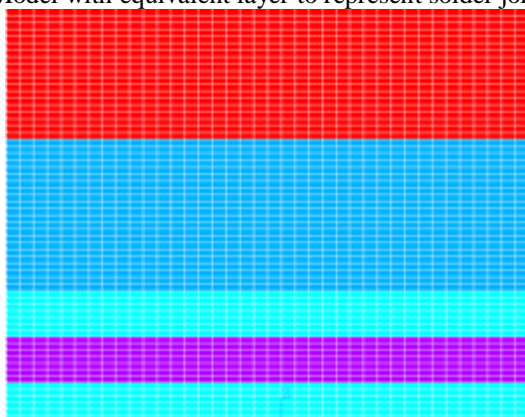**Figure no 3:** Complete model with solder joint and underfill
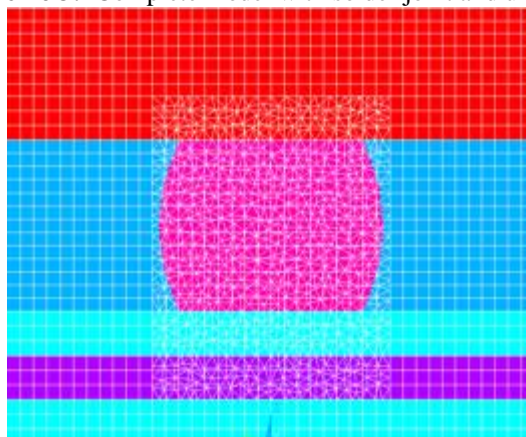
The model provides the control over the geometry of the embedded object and allows the addition of an offset, as shown in Figure no 4

Figure no 4: Tube with an offset

Figure no 5: Model with equivalent layer to represent solder joint and underfill

For the model using the equivalent layer, the model was created without the embedded solder joint, as shown in Figure no 5.

For all the models, a constant temperature of 373K was applied on the laminate and a thermal flux was applied on the die. The thermal flux applied on the model was evolved in order to keep the temperature of the die similar in all cases, and its amplitude was similar to what can be used in processes such as thermocompression [14].

Table no 1 presents the different parameters used for the model. Table no 1 also presents the default values used when studying the influence of another parameter

Table no 1: Parameters used for the model

Parameter	Default value
Die conductivity (W/(m.K))	150
Laminate conductivity (W/(m.K))	150
solder joint conductivity (W(m.K))	390
Underfill conductivity (W/(m.K))	0.26
Die thickness (μm)	50
Laminate thickness (μm)	50
Solder joint and underfill thickness (μm)	55
Solder joint contact surface diameter (μm)	20 to 80
Die and laminate x length (μm)	200
Die and laminate y length (μm)	200
Solder joint volume (μm^3) for respectively a cylindrical interconnect diameter of 20μm, 30μm, 40μm, 50μm, 60μm, 70μm and 80μm	17279, 28877, 69115, 107992, 155508, 211664 and 276460

V. Evaluation Of The Existing Simplified Models

At first we have compared the existing simplified models (7) with the detailed model with solder joint. This was done by comparing the temperatures of the die for the detailed model with the solder joint and the existing simplified models, with both models having the same boundary conditions.

For the example used in Figure no 6, the volume added to the simple cylindrical tube was 40%, to obtain a solder joint with a shape resembling a truncated sphere (Figure no 3). The relative differences in calculated temperatures was found to be between 6 and 8% for a range of ε between 0.1 and 0.35. These differences, presented in Figure no 6, show that the values of ψ provided by the literature are not accurate for complex geometries, thus the need for new values.

Figure no 6: Comparison of temperature between the complete model and the model with the conductivity of the equivalent layer obtained with literature formula
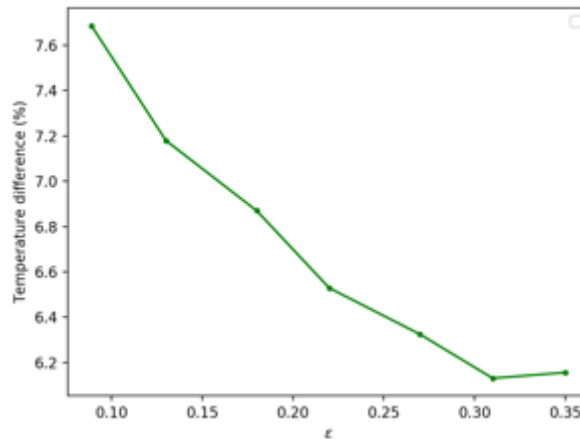

VI. Results And Discussion

The results obtains by modifying the parameters presented in Table no 1 are presented below.

In each case, the starting point was the geometry of a cylindrical interconnect for seven diameters (20μm, 30μm, 40μm, 50μm, 60μm, 70μm, 80μm), which give the seven volumes listed in Table no 1. One parameter at a time was then modified to evaluate the impact of the change of that parameter.

In the first place we assess the impact of the thickness of the underfill and solder joint, while the contact surface and the geometry of the solder joint is kept constant, with a 30% increase of the volume relative to the cylindrical tube. The thickness influences more the value of ψ when ε is small: the higher the thickness, the higher is ψ. When the value of ε increases, the thickness has less influence (Figure no 7)

Figure no 7: Variation of the thickness of the underfill
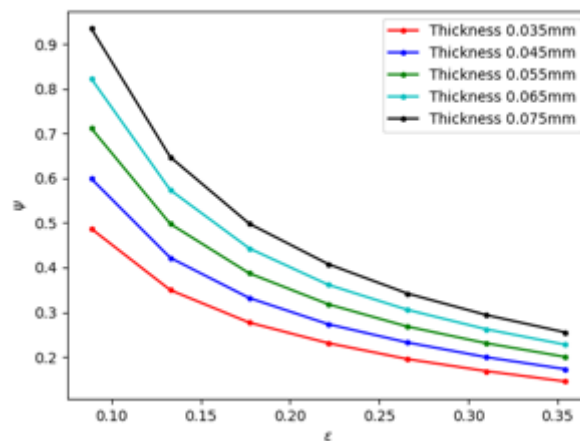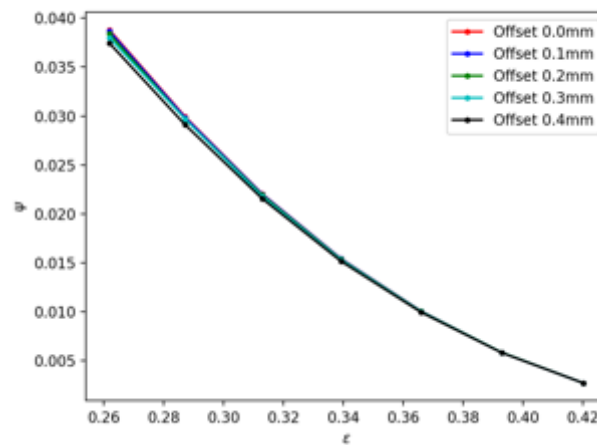

In the second place we studied the impact of the volume variation of the solder joint, while keeping the thickness and contact surface constant. We start from a tube and then we increase the equatorial diameter by increasing the volume, so we get closer to the geometry of a real solder joint. The value of ψ decreases with the added volume and increased sphericity (Figure no 8).

Figure no 8: Variation of the volume of the solder joint from a cylindrical tube
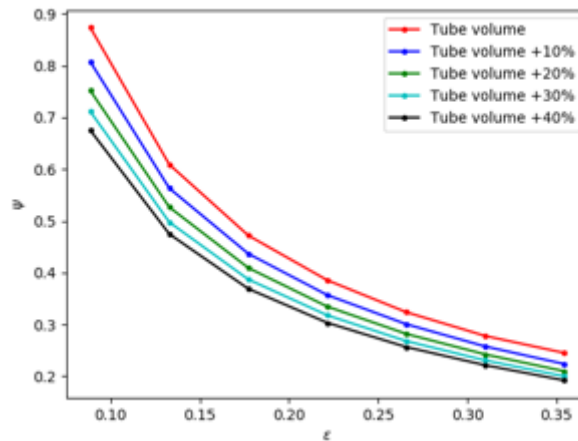
In the third place we study the impact of an offset on the solder joint, while keeping the thickness and volume of the solder joint constant. The variation of the offset of the solder joint has no significant influence on the value of ψ (Figure no 9).

Figure no 9: Variation of the offset of the tube.

In the fourth place we studied the impact of the difference of conductivity between the solder joint and the underfill. α is the ratio of the conductivity of the underfill to the conductivity of the solder joint. The value of ψ decreases when α increases (which is equivalent to the increase of the conductivity of the underfill), especially for low value of ε (Figure no 10).

**Figure no 10:** Variation of α. The first curve (red) is for a ratio of 0.00667
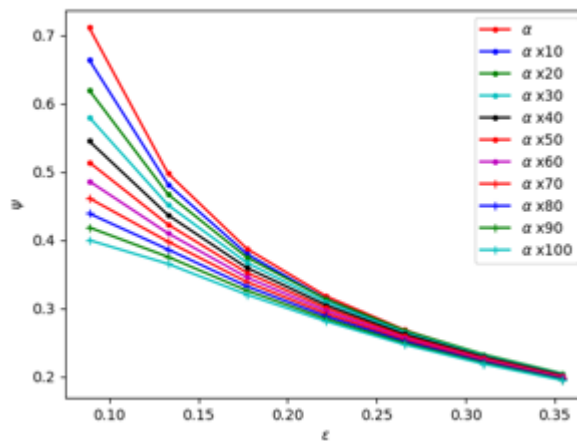
In the fifth place, we studied the impact of the area density of the solder joints by modifying the planar dimensions of the section of die, underfill and laminate (the density decreases when the dimensions of the die and of the laminate increase), while keeping the contact surface with solder joint constant. The value of ψ decreases when the dimensions of the die and laminate on which the thermal flux is imposed increases (Figure no 11).

Figure no 11: Variation of the dimensions of the die and laminate
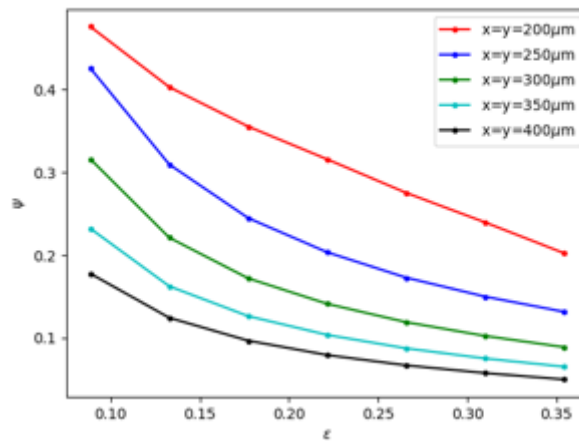
For all the models, regardless of which parameter was tested, when ε increases the value of ψ decreases (Figure no 7 to no 11).

The new ψ calculated using the complete model was then used to calculate the value of the equivalent layer conductivity, to compute the temperatures relative errors found at the die interface.

Figure no 12: Comparison of the temperature from the complete model and the temperature from the model with the conductivity of the equivalent layer obtained from the updated flux model tube
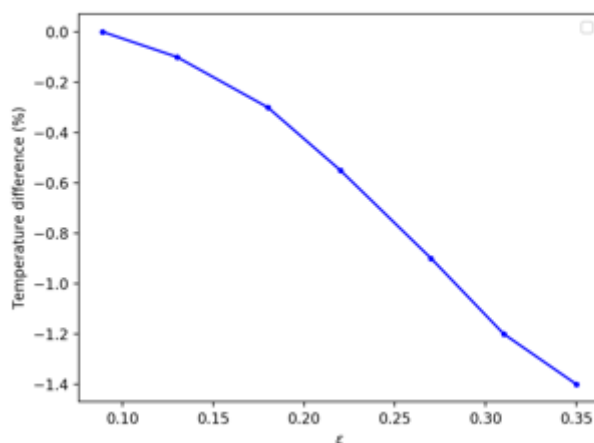
VII. Table of Results

The values of ψ found while studying the different parameters influencing ψ are described in the following tables. The data have been adimensionalized to be easily used in numerical studies (see Table no 1 for the initial geometry).

Variation Of The Thickness Of The Underfill

Table no 2-6: Thickness variation

Thickness -36%	
ε	ψ
0.090	0.490
0.133	0.350
0.177	0.277
0.222	0.231
0.266	0.195
0.310	0.168
0.354	0.150

Thickness -18%	
ε	ψ
0.090	0.600
0.133	0.422
0.177	0.332
0.222	0.273
0.266	0.232
0.310	0.199
0.354	0.173

Initial thickness	
ε	ψ
0.090	0.710
0.133	0.498
0.177	0.387
0.222	0.318
0.266	0.268
0.310	0.231
0.354	0.200

Thickness +18%

ε	ψ
0.090	0.820
0.133	0.573
0.177	0.443
0.222	0.361
0.266	0.305
0.310	0.262
0.354	0.227

Thickness +36%

ε	ψ
0.090	0.930
0.133	0.647
0.177	0.498
0.222	0.408
0.266	0.342
0.310	0.294
0.354	0.255

Variation Of The Volume Of The Solder Joint

Table no 7-11: Volume variation

Initial volume

ε	ψ
0.090	0.870
0.133	0.609
0.177	0.472
0.222	0.385
0.266	0.324
0.310	0.278
0.354	0.245

Initial volume +10%

ε	ψ
0.090	0.810
0.133	0.563
0.177	0.437
0.222	0.357
0.266	0.301
0.310	0.258
0.354	0.224

Initial volume +20%

ε	ψ
0.090	0.807
0.133	0.563
0.177	0.437
0.222	0.357
0.266	0.301
0.310	0.258
0.354	0.224

Initial volume +30%

ε	ψ

0.090	0.710
0.133	0.498
0.177	0.387
0.222	0.318
0.266	0.268
0.310	0.231
0.354	0.200

Initial volume +40%	
ε	ψ
0.090	0.680
0.133	0.475
0.177	0.369
0.222	0.303
0.266	0.256
0.310	0.221
0.354	0.192

Variation Of Conductivity Ratio

Table 12-22: Ratio of conductivity variation

Ratio of conductivity α	
ε	ψ
0.090	0.710
0.133	0.498
0.177	0.387
0.222	0.318
0.266	0.268
0.310	0.231
0.354	0.200
Ratio of conductivity αx10	
ε	ψ
0.090	0.660
0.133	0.481
0.177	0.379
0.222	0.314
0.266	0.265
0.310	0.229
0.354	0.199
Ratio of conductivity αx20	
ε	ψ
0.090	0.620
0.133	0.467
0.177	0.374
0.222	0.313
0.266	0.267
0.310	0.232
0.354	0.204
Ratio of conductivity αx30	
ε	ψ
0.090	0.580
0.133	0.451

0.177	0.367
0.222	0.309
0.266	0.264
0.310	0.231
0.354	0.203

Ratio of conductivity αx40

ε	ψ
0.090	0.550
0.133	0.436
0.177	0.359
0.222	0.305
0.266	0.262
0.310	0.229
0.354	0.202

Ratio of conductivity αx50

ε	ψ
0.090	0.510
0.133	0.423
0.177	0.352
0.222	0.300
0.266	0.259
0.310	0.227
0.354	0.200

Ratio of conductivity αx60

ε	ψ
0.090	0.490
0.133	0.410
0.177	0.345
0.222	0.296
0.266	0.256
0.310	0.225
0.354	0.199

Ratio of conductivity αx70

ε	ψ
0.090	0.460
0.133	0.398
0.177	0.338
0.222	0.292
0.266	0.254
0.310	0.223
0.354	0.198

Ratio of conductivity αx80

ε	ψ
0.090	0.440
0.133	0.386
0.177	0.332
0.222	0.288
0.266	0.251
0.310	0.222
0.354	0.197

Ratio of conductivity αx90

ε	ψ
0.090	0.420
0.133	0.375
0.177	0.326
0.222	0.285
0.266	0.249
0.310	0.220
0.354	0.195

Ratio of conductivity α x100

ε	ψ
0.090	0.400
0.133	0.365
0.177	0.320
0.222	0.281
0.266	0.246
0.310	0.218
0.354	0.194

VIII.   Conclusion

We have shown than when the geometry of the model is closer to the geometry of an actual solder joint than to the geometry of a cylinder, the results obtained from previous models published in the literature deviate from the real values. We have shown that the thickness of the underfill, the volume of the solder joint, the ratio between the conductivity of the solder joint and the conductivity of the underfill and the density of the solder joint influence the value of ψ. We have shown that adding an offset to the solder joint does not influence much the value of ψ

Acknowledgments

References

[1].   H. Clauberg, A. Rezvani, E. Galipeau, M. Wasserman, T. Colosimo, G. Frick, D. Buergi and B. Chylak, "Advanced Thermocompression Flip Chip Bonding", 2014 IEEE 16th Eectronics Packaging Technology Conference (EPTC), 2014, pp. 492-495
[2].   K.A. De Las Alas, C. Ison, J.O. Rivera, R. De La Cruz, R. Aguares, D. Vyas, T. Nguyen, M. Bailon-Sominac, "Temperature and Humidity Stress Failure on Copper Pillar (CuP) Flip Chip Package Device", 2017 IEEE 24th International Symposium on the Physical and Failure Analysis of Integrated Circuits (IPFA), 1-4 Jul, 2017
[3].   V. Smet, T-C. Huang B. Singh, V. Sundaram, P. M. Raj, R. Tummala, "Interconnection Materials, Process and Tools for Fine-pitch Panel Assembly of Ultra-thin Glass Substrates", IEEE Electronic Components and Technology Conference, 2015, pp. 475-483
[4].   H.Y. Yang, D. Pinjala, Y.K. Joshi, T.N. Wong, K.C. Toh, "Thermal Modelinf and Design of Liquid Cooled Heat Sink Assembled with Flip-Chip Ball Array Packages", 53rd Electric Components and Technology Conference, 2003
[5].   M. M. Yovanovich, V. W. Antonetti, "Application of thermal contact resistance theory to electronic packages", chapter 2 in 'Advances in thermal modeling of electronic components and systems', vol. 1, A. Bar-Cohen and A. D. Kraus, eds, New York : Hemisphere Publishing Corporation, 1988
[6].   K.J. Negus, M.M. Yovanovich, J. V. Beck, "On the Non-Dimensionalization of Construction Resistance for Semi-Infinite Heat Flux Tubes", ASME Journal of Heat Transfer, Vol. 111, 1989
[7].   J.L. Lau, J.L. Prince, W. Nakayama, C.P. Wong, "Electronic Packaging: Design, Materails, Process and Reliability, McGraw-Hill, 1998, pp. 121-123
[8].   G. Maranza, I. Perry, D. Maillet, S. Raël, "Design optimization of a spreader heat sink for power electronics", International Journal of Thermal Sciences 43, January 2004, pp. 21-29
[9].   W.M. Hannon, T.A. Barr, S.T. Froelich, "Rolling-Element Bearing Heat Transfer: Part III – Experimental Validation", Journal of Tribology 137, July 2015
[10].   S. Yang, J.S. Chalfant, J.C. Ordonez, J.A. Khan, C. Li, I. Cvetkovic, J.V.C. Vargas, M.B. Chagas, Y. Xu, R.P. Burgos, D. Boroyevich, "Shipboard PEBB Cooling Strategies", Conference: 2019 IEEE Electric Ship Technologies Symposium, Arlington, VA, USA, August 2019
[11].   ST. Lu, J-Y. Juang, H-C. Cheng, "Effects of Bonding Parameters on the Reliability of Fine-Pitch Cu/Ni/SnAg Micro-Bump Chip-to-Chip Interconnection for Three-Dimensional Chip Stacking", IEEE Transaction On Device And Material Reliability, Vol. 12, No. 2, June 2012
[12].   J. Sylvestre, "Integrated Modeling of C4 Interconnects," 2007 Proceedings 57th Electronic Components and Technology Conference, pp. 1084–1090, 2007
[13].   « Surface Evolver. » [En ligne]. Available on: http://facstaff.susqu.edu/brakke/evolver/evolver.html. [Consulted le : 10-aug-2019]
[14].   N. Malik, K. Schjølberg-Henriksen, E. Poppe, M.M.Visser Taklo, T.G. Finstad, "Al-Al thermocompression bonding for wafer-level MEMS sealing", ELSVIER, Sensors and Actuators A: Physical, pp. 115-120, 2014